

Single-particle Excitation Spectra of C_{60} Molecules and Monolayers

Fei Lin,¹ Erik S. Sørensen,² Catherine Kallin,² and A. John Berlinsky²

¹*Department of Physics, University of Illinois at Urbana-Champaign, Urbana, Illinois 61801, USA*

²*Department of Physics and Astronomy, McMaster University, Hamilton, Ontario, Canada L8S 4M1*

(Dated: March 23, 2022)

In this paper we present calculations of single-particle excitation spectra of neutral and three-electron-doped Hubbard C_{60} molecules and monolayers from large-scale quantum Monte Carlo simulations and cluster perturbation theory. By a comparison to experimental photoemission, inverse photoemission, and angle-resolved photoemission data, we estimate the intermolecular hopping integrals and the C_{60} molecular orientation angle, finding agreement with recent X-ray photoelectron diffraction (XPD) experiments. Our results demonstrate that a simple effective Hubbard model, with intermediate coupling, $U = 4t$, provides a reasonable basis for modeling the properties of C_{60} compounds.

PACS numbers: 73.61.Wp, 78.20.Bh, 02.70.Uu

I. INTRODUCTION

C_{60} compounds occupy a unique place within the pantheon of high-temperature superconductors.^{1,2,3,4,5,6} One would not normally expect such high transition temperatures (30-40K) to arise from the conventional phonon mechanism of superconductivity. However, the unusual molecular structure of these compounds results in higher frequency phonons and stronger couplings than are possible in typical elemental compounds and alloys.⁷ In a similar way, the effects of electron-electron interactions on these molecules are more complex and, it has been argued,^{8,9} could also provide the mechanism for attractive pairing. There is general agreement that the attractive mechanism is intramolecular, i.e., it arises from intramolecular vibrations or from Coulomb correlations on a molecule or, perhaps most likely, from a combination of the two effects.¹⁰ This intramolecular attraction, together with the narrow bands and correspondingly large density of states (DOS) for intermolecular hopping, is believed to account for the observed high transition temperatures. The two contrasting theoretical approaches, which emphasize either phonons or Coulomb interactions, can be roughly characterized as an LDA electronic structure coupled to Jahn-Teller phonons, compared to a Hubbard model of the C_{60} molecule with tight-binding intermolecular hopping.

Recently Yang *et al.*¹¹ reported angle-resolved photoemission (ARPES) and LDA calculations of the band structure of two-dimensional (2D) hexagonal monolayers of C_{60} and K_3C_{60} on the surface of silver, and Wehrli *et al.*¹² have proposed an electron-phonon mechanism to explain the DOS observed in Yang *et al.*'s study as well as spectra from earlier experiments.^{13,14,15} Since their calculations do not capture the distinctive correlation effects of the Hubbard model within a molecule, it is of interest to examine how the DOS and other properties are affected by such correlations.

In this paper, we calculate the photoemission spectra (PES) and inverse photoemission spectra (IPES) of 2D hexagonal C_{60} monolayers including the strong,

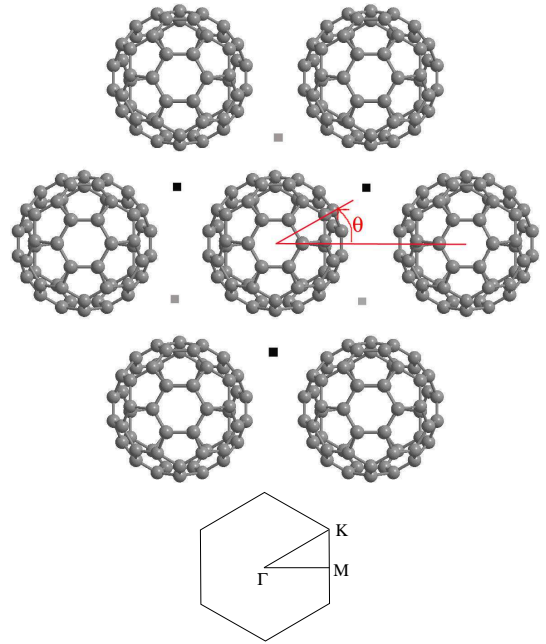


FIG. 1: (Color online) 2D hexagonal monolayer of identically oriented C_{60} molecules (lattice constant $a = 10.02\text{\AA}$ for the superlattice¹¹) and its corresponding first Brillouin zone (BZ). The definition of the molecular rotation angle θ is the same as in the caption of Fig. 4 of Ref. 11, which is defined by two lines, both projected onto the plane of the layer, one from a molecular center to a NN molecular center, as shown, and the other from a molecular center through a pentagon face center. $\theta = 0^\circ$ when these two lines coincide. Counterclockwise rotation of the molecule corresponds to a positive rotation angle. For K_3C_{60} , the black squares represent two K^+ ions, one above the other, while gray ones denote a single K^+ ion.¹¹

atomic, on-site electron-electron Coulomb interaction U within a single molecule. The calculation is performed by cluster perturbation theory (CPT)^{16,17} using quantum Monte Carlo (QMC) data.¹⁸ This method, which we call QMCPT, is ideally suited to calculating the electronic properties of solids composed of complex units

such as fullerene molecules. To distinguish, we shall refer to the standard CPT approach^{16,17} as EDCPT since it uses exact diagonalization (ED) results. By comparing the calculated single-particle excitation spectra, for intermediate interaction strength, $U = 4t$, with experimental data,^{11,19} we can estimate the intermolecular hopping integrals t' and the molecular orientation angle, θ , which are useful for an effective Hubbard model Hamiltonian description of C_{60} compounds. From the best fit parameters, we find a rotation angle of $\theta = 64^\circ$ (as defined in Fig. 1, and assuming that the C_{60} molecules are all oriented identically) which is consistent with experimental measurements.^{11,20}

II. MODEL

The Hamiltonian for the 2D hexagonal C_{60} superlattice is given by

$$H = H_0 + V, \quad (1)$$

$$H_0 = \sum_I H_0^I, \quad (2)$$

where

$$H_0^I = - \sum_{\langle Ii, Ij \rangle \sigma} t_{ij} (c_{i\sigma}^\dagger c_{j\sigma} + h.c.) + U \sum_{i \in I} n_{i\uparrow} n_{i\downarrow} \quad (3)$$

is the Hubbard model on the I th C_{60} molecule, and

$$V = - \sum_{\langle Ii, Jj \rangle \sigma} (t' \alpha_{Ii, Jj} + t_{Ii, Jj}^{\text{ind}}) (c_{Ii\sigma}^\dagger c_{Jj\sigma} + h.c.) \quad (4)$$

is the hopping Hamiltonian between a pair of carbon (C) atoms i and j on two nearest neighbor (NN) C_{60} molecules I and J , respectively. The operator notations are standard for the usual Hubbard model. Inside the molecule U is the on-site Coulomb interaction energy for two electrons on the same C atom, and t_{ij} is the hopping integral between two NN carbon atoms. A *molecular* U , parameterizing the interaction energy for two electrons on the same C_{60} molecule, and hence distinct from our atomic U , is also discussed in the literature. See for instance Ref. 19. For the C_{60} molecule, there are two kinds of bonds between NN sites: $t_{ij} = t$ for single bonds (1.46\AA), and $t_{ij} = 1.2t$ for double bonds (1.40\AA). We set $t = 2.72\text{eV}$ according to Ref. 21. The value of the on-site Coulomb energy, U , is taken to be $U = 4t$, an intermediate coupling value for which the sign problem for the single-molecule QMC is manageable.²²

The shortest distance between two C_{60} molecules is about 3.0\AA . The relative sizes of the direct hopping integrals $\alpha_{Ii, Jj}$ between two C atoms on two NN molecules are given by²³

$$\alpha_{Ii, Jj} = [V_\sigma(d) - V_\pi(d)] (\hat{\mathbf{R}}_{Ii} \cdot \hat{\mathbf{d}}) (\hat{\mathbf{R}}_{Jj} \cdot \hat{\mathbf{d}}) + V_\pi(d) (\hat{\mathbf{R}}_{Ii} \cdot \hat{\mathbf{R}}_{Jj}), \quad (5)$$

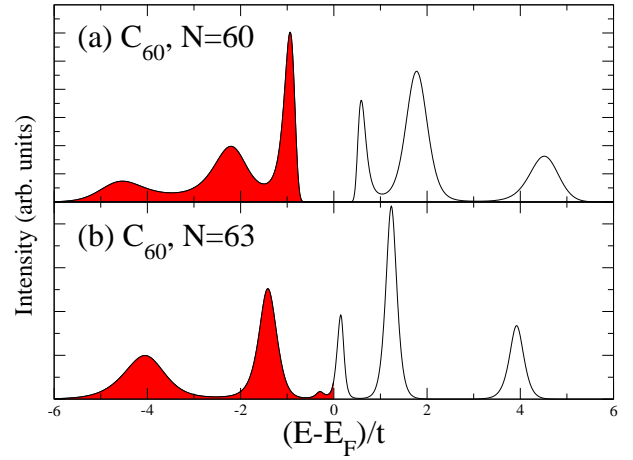


FIG. 2: (Color online) DOS of (a) C_{60} and (b) C_{60}^{3-} single molecules from QMC and MEM for $U = 4t$ and $\beta t = 10$. A total of 465 and 620 bins of space-time Green's functions are collected for C_{60} and C_{60}^{3-} , respectively, for MEM analysis. Each bin is an average over 100 space-time Green's functions, which are collected after each QMC sweep over the whole space-time lattice.

where $\hat{\mathbf{R}}$ is a unit vector along radial direction, $\hat{\mathbf{d}} = \mathbf{d}/d$ is a unit vector pointing from atom Ii to Jj , and

$$V_\sigma(d) = -4V_\pi(d) = \frac{d}{d_0} \exp[-(d - d_0)/L], \quad (6)$$

with $L = 0.505\text{\AA}$, and $d_0 = 3.0\text{\AA}$.²³ We leave the overall prefactor t' as a parameter to be determined later.

We see from Fig. 1 that for K_3C_{60} the C_{60} molecules are separated by K^+ ions, either two ions, one above the other or single ions. The indirect hopping between C_{60} molecules via K^+ ions is thus of comparable importance to that of the direct C-C hopping integrals. Expressions for the indirect hopping between C atoms via the K^+ ions are given by²⁴

$$t_{Ii, Jj}^{\text{ind}} = \sum_\gamma \frac{t_{Ii, \gamma} t_{Jj, \gamma}}{\epsilon_C - \epsilon_K}, \quad (7)$$

where $\epsilon_C - \epsilon_K = -4\text{eV}$ is the energy difference between a C atom and K^+ ion, $\gamma = 1, \dots, 9$ is K^+ index, and the C-K hopping integral is given by

$$t_{Ii, \gamma} = 1.84D \frac{\hbar^2}{m d^2} e^{-3(d - R_{\text{min}})}, \quad (8)$$

where d is C-K separation, m is electron mass, R_{min} is the shortest C-K separation for a given K^+ and C_{60} molecule, and $D = 0.47$.²⁴ We take the indirect hopping matrix elements to be fixed while the direct hopping matrix elements scale with the fitting parameter t' . For the value of t' used to fit the ARPES data, we find that the largest direct hopping matrix elements are substantially larger than the indirect hopping matrix elements.

We note that our model Hamiltonian, given by Eqs. (2)-(4), neglects both the long-range Coulomb interactions and the effect of the silver substrate, both of which would be difficult to include in QMC calculations. One would expect the long-range Coulomb interaction to increase the effective molecular U . On the other hand, the silver substrate, as well as the other molecules, will screen this interaction and, consequently, these two effects may partially cancel. In any case, we will see below that the simple Hubbard model and parameters employed here yield results in generally good agreement with experiment.

III. RESULTS

A. Single Molecule DOS

We begin by considering results for a single C_{60} molecule. QMC simulations were used to calculate the imaginary-time Green's functions for C_{60} and C_{60}^{3-} molecules, based on the single-molecule Hamiltonian, H_0 and standard QMC^{25,26,27} for given values of t and U . The QMC step for the single molecule is by far the most time-consuming part of the calculation. The maximum entropy method (MEM) was then used to analytically continue the imaginary-time Green's functions to real frequency,²⁸ which gives the single molecule DOS shown in Fig. 2 for $T = 0.1t$. From the figure, we see that neutral C_{60} is an insulator with an energy gap about $1.05t$ or 2.86eV . The presence of this gap is not surprising since neutral C_{60} has a filled shell with a sizable excitation gap even for $U = 0$. In fact the gap obtained by extended Huckel calculations for the neutral model is also about $1t$, although the correlations for that case are very different than for $U = 4t$. For the C_{60}^{3-} molecule, the Fermi energy lies in a region of non-zero density of states.

B. QMCPT for 2D Square Lattice

The remaining perturbative part of the QMCPT calculation is, by comparison, very economical. It uses the single molecule Green's functions calculated above to construct any superlattice Green's functions, incorporating the effect of the intermolecular hopping Hamiltonian, V , and different molecular orientations with negligible additional computational effort. This method has been applied to the simpler case of the 2D Hubbard model on a square lattice, which is metallic for $U = 0$ but which develops an insulating Mott-Hubbard gap for sufficiently large U . The "cluster" in this case is a small unit of the lattice which can be treated either by QMC or by exact diagonalization. Results for $U = 8t$, obtained by QMCPT and by EDCPT, based on a 3×4 cluster of sites,¹⁸ are shown in Fig. 3.

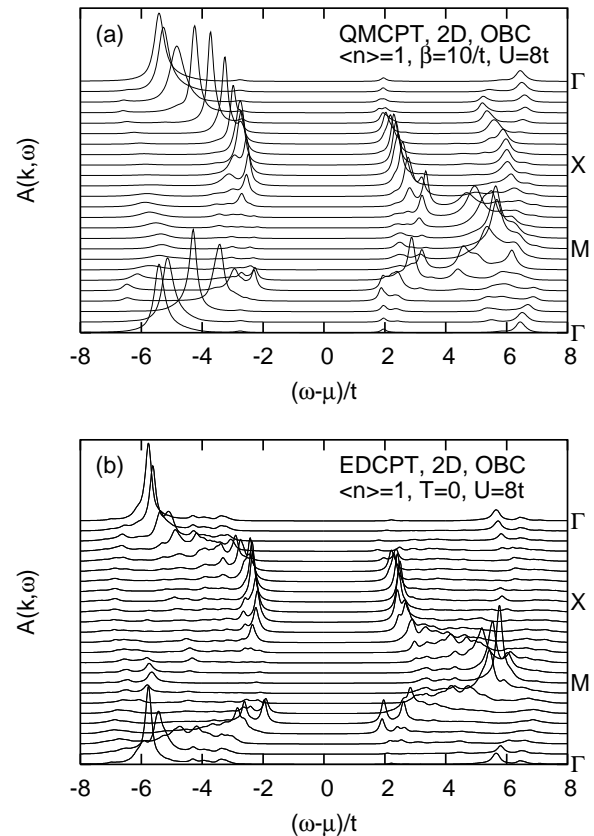


FIG. 3: Single particle spectral functions of a 2D Hubbard model from (a) QMCPT and (b) EDCPT with open boundary conditions. The cluster is of dimension 3×4 . The two methods predict very similar single-particle excitation energies and energy gaps. Note that special \mathbf{k} points Γ, M, X are for a 2D square lattice, different from those in Fig. 1.

C. Monolayer DOS

Next we consider the case of C_{60} monolayers. For these calculations we use values of t' and the orientation angle θ which are obtained by fitting photoemission and diffraction data as will be discussed below. We show the DOS for monolayers of both C_{60} and K_3C_{60} , in panels (b) and (c) of Fig. 4. Also shown for comparison, in panel (a) of Fig. 4, is the DOS for the same values of t' and θ , but for $U = 0$. The lattice of neutral C_{60} molecules is very different from the 2D square lattice of atomic sites, for which spectra are shown in Fig. 3, because the C_{60} molecule has an excitation gap as was shown in the top panel of Fig. 2. For $U = 0$ [(a) panel of Fig. 4], the C_{60} monolayer is a band insulator with a gap of about $0.5t$ which is about half the value for the single-molecule case because the bands above and below the gap are broadened by temperature effects and the intermolecular Hamiltonian V , thus reducing the gap. We see, from the (b) panel where $U = 4t$, that the effect of U is to enlarge the gap back to a value ($\sim 2.8\text{eV}$) slightly greater than $1t$

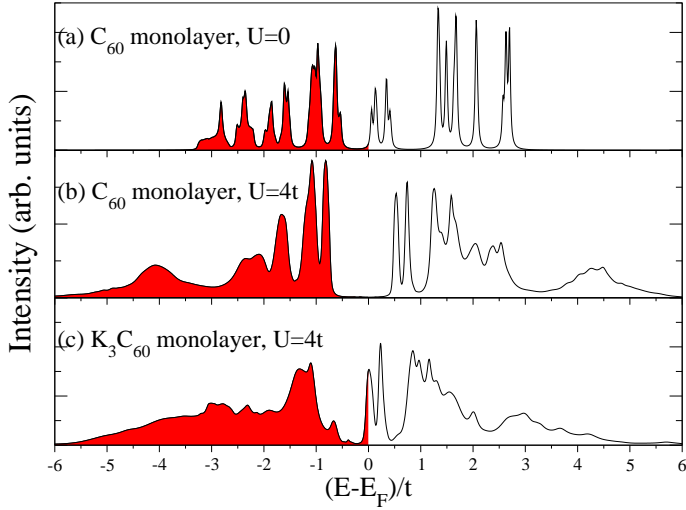


FIG. 4: (Color online) DOS of hexagonal (a) C_{60} monolayer with $U = 0$, (b) C_{60} monolayer with $U = 4t$, and (c) K_3C_{60} monolayer with $U = 4t$ from QMCPT calculations for $t' = -0.3t$ and $T = 0.1t$. Shaded areas are occupied by electrons.

due to short-range, Mott-Hubbard correlations. This gap value is comparable to the value of 2.3eV measured by Lof *et al.* in Ref. 19. Our calculated gap value may be somewhat larger than the experimental gap due to our neglect of the silver substrate, which may reduce the energy gap.²⁹ By contrast, for the case of K_3C_{60} [(c) panel] the monolayer remains metallic with its Fermi energy lying within a narrow conduction band (Fig. 4).

To determine the parameter t' and orientation angle θ , we vary t' and θ values in the QMCPT calculations. The resulting energy-momentum dispersion curves (along the ΓM direction) for the hexagonal monolayer of K_3C_{60} are then compared with the experimental one from ARPES.¹¹ We find that the best fit is obtained when $t' = -0.3t$ with a rotation angle $\theta = 64^\circ \pm 4^\circ$. From Fig. 5, we see that both the experimental and theoretical band widths are about 100meV. However the theoretical band dispersion in the k range $[-0.8, -0.6]\text{\AA}^{-1}$ is rather weak around the Fermi energy, while in the experimental dispersion figure, the band dispersion in that momentum range is much more obvious. We think that this results from two causes: First MEM has difficulty reconstructing the weak features of the band dispersion curve, and, second, the experimental scanning direction is not exactly along ΓM .¹¹ The above determined rotation angle $\theta = 64^\circ \pm 4^\circ$ is in good agreement with XPD structural data.²⁰

The densities of states in the lower two panels of Fig. 4 are directly comparable to the PES data (Fig. 1E in Ref. 11) of Yang *et al.*, we draw only the photoemission (PE) part of the calculated DOS together with the experimental PES data in Fig. 6. We see that the QMCPT results agree reasonably well with the PES data close to the Fermi energy, with approximately the same energy gaps for the C_{60} monolayer and similar peaks at the

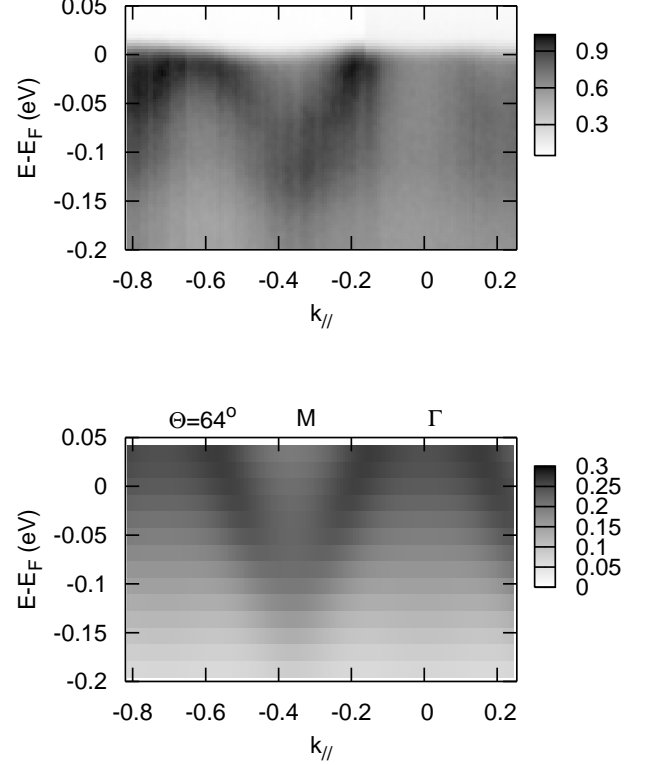


FIG. 5: Determination of NN molecular hopping integral t' and molecular orientation angle θ by comparing the experimental ARPES result¹¹ (upper panel) with the theoretical one (lower panel), which has $t' = -0.3t$ and molecular rotation angle $\theta = 64^\circ$. The energy unit has been converted to eV using $t = 2.72\text{eV}$. The momentum unit is \AA^{-1} .

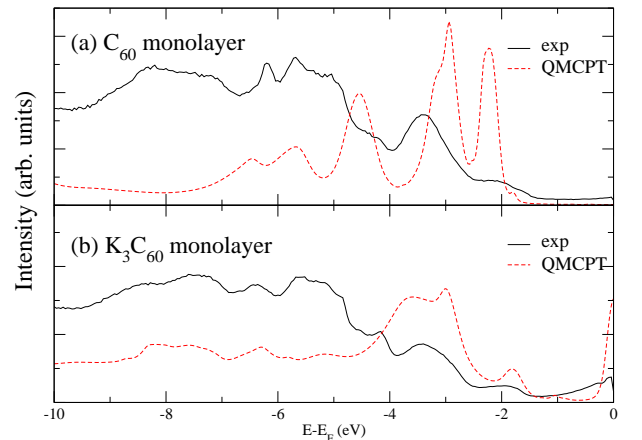


FIG. 6: (Color online) Comparison of DOS from QMCPT calculations and experimental PES data¹¹ for C_{60} (upper panel) and K_3C_{60} (lower panel) hexagonal monolayer. The QMCPT energy scale has been converted to electron volts by setting $t = 2.72\text{eV}$.

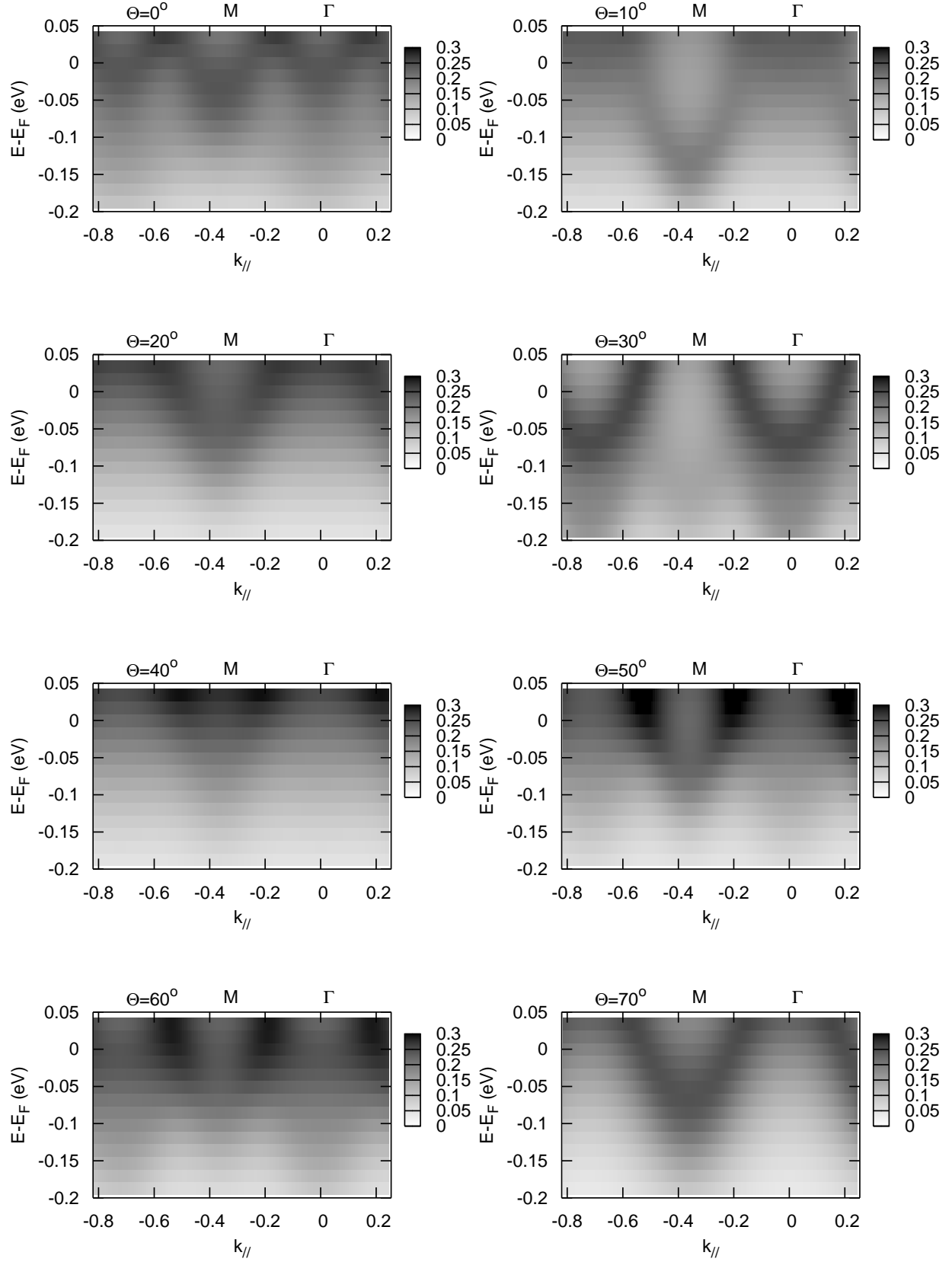


FIG. 7: Band dispersions along ΓM direction with different rotation angles θ for a 2D hexagonal K_3C_{60} superlattice from QMCPT calculations. The other parameters are fixed: $U = 4t$, $t' = -0.3t$, and $T = 0.1t$. The momentum unit is \AA^{-1} .

Fermi energy for the K_3C_{60} monolayer. In addition, we find small peaks at around -2eV and valleys at around -4eV for both theoretical and experimental PES curves. Thus, although we do not claim that $U = 4t$ corresponds to a fit to the data, this value of U is consistent with the PES data. Smaller or larger values of U would lead to smaller or larger values of the gap for neutral C_{60} monolayers. Unfortunately, to go beyond this by varying the value of U would, at present, require a prohibitively large amount of computer time.

We comment that the above-determined value of t' is consistent with earlier TB and LDA calculations²³, where Satpathy *et al.* found good agreement between TB and LDA band structure calculations for a fcc C_{60} lattice. The magnitudes of their TB hopping integrals between two nearest C atoms on two NN C_{60} molecules are, depending on the relative orientations of NN C_{60} molecules, in the range of $(0.50\text{eV}, 0.82\text{eV})$. From our calculation, the maximum C-C hopping integral between two NN C_{60} molecules is about 0.51eV (calculated from $t' \propto I_{i,j}$). Therefore, our estimated TB hopping integrals agree with Satpathy *et al.*'s calculations.

In our formalism, it is easy to explore the variation of the monolayer band structure with different C_{60} rotation angles θ . In fact it was necessary to do just this to determine the orientation which best fit the ARPES band structure. Fixing $t' = -0.3t$, we carry out QMCPT for C_{60} molecular rotation angles $\theta = 0, 10^\circ, \dots, 70^\circ$ for a K_3C_{60} monolayer. The band dispersions along the ΓM direction are shown in Fig. 7. We see that the band structure is quite sensitive to the molecular rotation angle θ . For example, at $\theta = 30^\circ$, the band is inverted with a band minimum at Γ and a maximum at M . At $\theta = 40^\circ$, the band becomes almost insulating. These are quite interesting, and might be verified by experiments if a way can be found to control the molecular orientation.

IV. CONCLUSION

To summarize we have calculated theoretical single-particle excitation spectra for single C_{60} and C_{60}^{3-} molecules as well as for hexagonal monolayers of C_{60} and

K_3C_{60} . The calculations were carried out by the QMCPT technique,^{16,17,18} using a Hubbard model for each molecule, and simple electron hopping between molecules of the 2D C_{60} superlattice. This new computational method is particularly well-suited to composite systems of fullerenes. Using a plausible value, $U = 4t$, for the on-site Coulomb interaction U , we fit the effective NN molecular hopping amplitude, t' , and the C_{60} molecular rotation angle θ to ARPES and XPD data. We find that the electronic spectra are extremely sensitive to the molecular orientation angle θ . With these fitted parameters, we find good agreement with photoemission data for the electronic density of states. The C-C hopping integrals between NN molecules obtained from the fits are consistent with earlier TB and LDA calculations.²³

The significance of the present calculations is to show that the electronic spectral data obtained so far are compatible with the relatively simple model of electronic correlations contained in the intramolecular Hubbard model with simple interball hopping, in much the same way as they have also been shown by others^{11,12} to be compatible with LDA/phonon calculations. Further measurements and calculations will be required in order to refine our understanding of the dominant correlations in these systems.

Acknowledgments

This project was supported by the Natural Sciences and Engineering Research Council (NSERC) of Canada, the Canadian Institute for Advanced Research (CIAR), and the Canadian Foundation for Innovation (CFI). FL was supported by US Department of Energy under award number DE-FG52-06NA26170. AJB and CK gratefully acknowledge the hospitality and support of the Stanford Institute for Theoretical Physics where part of this work was carried out. All the calculations were performed at SHARCNET supercomputing facilities. We thank Z.X. Shen and W.L. Yang for helpful discussions and for sending us the experimental data shown in Fig. 5 and 6. We also thank G.A. Sawatzky for helpful discussions.

- ¹ A. F. Hebard, M. J. Rosseinsky, R. C. Haddon, D. W. Murphy, S. H. Glarum, T. T. M. Palstra, A. P. Ramirez, and A. R. Kortan, *Nature* **350**, 600 (1991).
- ² M. J. Rosseinsky, A. P. Ramirez, S. H. Glarum, D. W. Murphy, R. C. Haddon, A. F. Hebard, T. T. M. Palstra, A. R. Kortan, S. M. Zahurak, and A. V. Makhija, *Phys. Rev. Lett.* **66**, 2830 (1991).
- ³ K. Tanigaki, T. W. Ebbesen, S. Saito, J. Mizuki, J. S. Tsai, Y. Kubo, and S. Kuroshima, *Nature* **352**, 222 (1991).
- ⁴ K. Holczer, O. Klein, S. M. Huang, R. B. Kaner, K. J. Fu, R. L. Whetten, and F. Diederich, *Science* **252**, 1154 (1991).

- ⁵ S. P. Kelty, C. Chen, and C. M. Lieber, *Nature* **352**, 223 (1991).
- ⁶ R. M. Fleming, A. P. Ramirez, M. J. Rosseinsky, D. W. Murphy, R. C. Haddon, S. M. Zahurak, and A. V. Makhija, *Nature* **352**, 787 (1991).
- ⁷ M. Schluter, M. Lannoo, M. Needels, G. A. Baraff, and D. Tománek, *Phys. Rev. Lett.* **68**, 526 (1992).
- ⁸ S. Chakravarty, M. P. Gelfand, and S. Kivelson, *Science* **254**, 970 (1991).
- ⁹ G. Baskaran and E. Tosatti, *Curr. Sci.* **61**, 33 (1991).
- ¹⁰ J. E. Han, O. Gunnarsson, and V. H. Crespi, *Phys. Rev. Lett.* **90**, 167006 (2003).

- ¹¹ W. L. Yang, V. Brouet, X. J. Zhou, H. J. Choi, S. G. Louie, M. L. Cohen, S. A. Kellar, P. V. Bogdanov, A. Lanzara, A. Goldoni, et al., *Science* **300**, 303 (2003).
- ¹² S. Wehrli, T. M. Rice, and M. Sigrist, *Phys. Rev. B* **70**, 233412 (2004).
- ¹³ C. T. Chen, L. H. Tjeng, P. Rudolf, G. Meigs, J. E. Rowe, J. Chen, J. P. McCauley, A. B. Smith, A. R. McGhie, W. J. Romanow, et al., *Nature* **352**, 603 (1991).
- ¹⁴ P. J. Benning, F. Stepniak, D. M. Poirier, J. L. Martins, J. H. Weaver, L. P. F. Chibante, and R. E. Smalley, *Phys. Rev. B* **47**, 13843 (1993).
- ¹⁵ R. Hesper, L. H. Tjeng, A. Heeres, and G. A. Sawatzky, *Phys. Rev. B* **62**, 16046 (2000).
- ¹⁶ D. S  n  chal, D. Perez, and M. Pioro-Ladri  re, *Phys. Rev. Lett.* **84**, 522 (2000).
- ¹⁷ D. S  n  chal, D. Perez, and D. Plouffe, *Phys. Rev. B* **66**, 075129 (2002).
- ¹⁸ F. Lin, E. S. S  rensen, C. Kallin, and A. J. Berlinsky, in *HPCS* (IEEE Computer Society, 2006), p. 27.
- ¹⁹ R. W. Lof, M. A. van Veenendaal, B. Koopmans, H. T. Jonkman, and G. A. Sawatzky, *Phys. Rev. Lett.* **68**, 3924 (1992).
- ²⁰ A. Tamai, A. P. Seitsonen, R. Fasel, Z. X. Shen, J. Osterwalder, and T. Greber, *Phys. Rev. B* **72**, 085421 (2005).
- ²¹ S. Satpathy, *Chem. Phys. Lett.* **130**, 545 (1986).
- ²² F. Lin, J.   makov, E. S. S  rensen, C. Kallin, and A. J. Berlinsky, *Phys. Rev. B* **71**, 165436 (2005).
- ²³ S. Satpathy, V. P. Antropov, O. K. Andersen, O. Jepsen, O. Gunnarsson, and A. I. Liechtenstein, *Phys. Rev. B* **46**, 1773 (1992).
- ²⁴ O. Gunnarsson, S. C. Erwin, E. Koch, and R. M. Martin, *Phys. Rev. B* **57**, 2159 (1998).
- ²⁵ J. E. Hirsch, *Phys. Rev. B* **31**, 4403 (1985).
- ²⁶ J. E. Hirsch, *Phys. Rev. B* **38**, R12023 (1988).
- ²⁷ S. R. White, D. J. Scalapino, R. L. Sugar, E. Y. Loh, J. E. Gubernatis, and R. T. Scalettar, *Phys. Rev. B* **40**, 506 (1989).
- ²⁸ M. Jarrell and J. E. Gubernatis, *Phys. Rep.* **269**, 133 (1996).
- ²⁹ R. Hesper, L. H. Tjeng, and G. A. Sawatzky, *Europhys. Lett.* **40**, 177 (1997).